

Activation of Akt as a Mechanism for Tumor Immune Evasion

Kyung Hee Noh¹, Tae Heung Kang¹, Jin Hee Kim¹, Sara I Pai², Ken Y Lin³, Chien-Fu Hung⁴, T-C Wu⁴⁻⁷ and Tae Woo Kim¹

¹Division of Infection and Immunology, Graduate School of Medicine, Korea University, Seoul, South Korea; ²Otolaryngology/Head and Neck Surgery, The Johns Hopkins Medical Institutions, Baltimore, Maryland, USA; ³Gynecology & Reproductive Sciences, Department of Obstetrics, Yale University School of Medicine, New Haven, Connecticut, USA; ⁴Department of Pathology, The Johns Hopkins Medical Institutions, Baltimore, Maryland, USA; ⁵Department of Obstetrics and Gynecology, The Johns Hopkins Medical Institutions, Baltimore, Maryland, USA; ⁶Department of Oncology, The Johns Hopkins Medical Institutions, Baltimore, Maryland, USA; ⁷Department of Molecular Microbiology and Immunology, The Johns Hopkins Medical Institutions, Baltimore, Maryland, USA

Immune evasion is an important reason why the immune system cannot control tumor growth. To elucidate the mechanism for tumor immune evasion, we generated an immune-resistant human papillomavirus type 16 (HPV-16) E7-expressing tumor cell line by subjecting a susceptible tumor cell line to multiple rounds of *in vivo* immune selection with an E7-specific vaccine. Comparison of parental and immune-resistant tumors revealed that Akt is highly activated in the immune-resistant tumors. Retroviral transfer of a constitutively active form of Akt into the parental tumor significantly increased its resistance against E7-specific CD8⁺ T-cell mediated apoptosis. The observed resistance against apoptosis was found to be associated with the upregulation of anti-apoptotic molecules. We also observed that intratumoral injection of an Akt inhibitor enhanced the therapeutic efficacy of E7-specific vaccine or E7-specific CD8⁺ T-cell adoptive transfer against the immune-resistant tumors. Thus, our data indicate that the activation of PI3K/Akt pathway represents a new mechanism of immune escape and has important implications for the development of a novel strategy in cancer immunotherapy against immune-resistant tumor cells.

Received 6 August 2008; accepted 17 October 2008; published online 23 December 2008. doi:10.1038/mt.2008.255

INTRODUCTION

Cancer immunotherapy has been reasonably successful in generating tumor-specific immune responses, leading to significant antitumor effects. However, in some cases, it is observed that the generation of tumor-specific immune responses does not translate into tumor regression in cancer patients.¹ One potential explanation is that tumors, with their abnormal patterns of gene expression and prolonged, insidious growth, can possibly influence and impair the immune system in many ways. Thus, it is important to focus on the molecular abnormalities of certain

tumors that may facilitate their ability to escape attack from the immune system.

To generate a suitable preclinical model to study the mechanisms of tumor immune evasion, we employed an *in vivo* selection strategy using a previously developed human papillomavirus type 16 (HPV-16) E7-expressing cancer cell line, called TC-1/P0, which has served as a preclinical tumor model for testing various E7-specific cancer immunotherapies.^{2,3} We have previously generated an HPV-16 E7-expressing vaccinia virus vaccine termed Vac-Sig/E7/LAMP-1, which encodes a fusion protein consisting of an endoplasmic reticulum signal sequence, HPV-16 E7 gene, and the transmembrane and cytoplasmic domains of lysosome-associated membrane protein-1 (LAMP-1).⁴ Vaccination with Vac-Sig/E7/LAMP-1 led to a substantial increase in both E7-specific CD8⁺ and CD4⁺ T-cell immune responses as compared to wild-type E7 vaccinia virus, preventing the growth of TC-1/P0 in 60–80% of immunized mice.²

Using the TC-1/P0 cell line and the Sig/E7/LAMP-1 vaccinia vaccine, we generated an immunoresistant tumor cell line, P3, from the TC-1/P0 parental tumors.⁵ Briefly, we immunized mice with Sig/E7/LAMP-1 vaccinia and challenged them with TC-1/P0 tumors. We then explanted an outgrowth tumor from the immunized mouse and expanded it *in vitro*. This escape variant cell line was designated P1 and was injected into a new group of mice immunized with Sig/E7/LAMP-1 vaccinia. A tumor from immunized mice was explanted and expanded *in vitro* into another cell line (P2). These repeated challenges with vaccine resistant tumor cells allowed us to perform an *in vivo* immune selection and resulted in increasing resistance to immunization. After three rounds of immune selection, we obtained the P3 cell line, which was completely resistant to the vaccine-induced immune response. Both the P0 and P3 cell lines grew with similar growth kinetics. However, when these cell lines were injected into mice immunized with Sig/E7/LAMP-1 vaccinia, P3 was developed palpable tumors in all challenged mice within 7 days, while only 2 out of 5 mice challenged with the P0 tumor cell developed tumors after several weeks. Thus, we were successfully

The first two authors contributed equally to this work.

Correspondence: T-C Wu, Department of Pathology, The Johns Hopkins University School of Medicine, CRB II Room 309, 1550 Orleans Street, Baltimore, Maryland 21231, USA. E-mail: wutc@jhmi.edu or Tae W Kim, Laboratory of Infection and Immunology, Graduate School of Medicine, Korea University, 516 Gojan-1 Dong, Ansan-Si, Gyeonggi-Do 425-707, South Korea. E-mail: twkim0421@korea.com

able to generate an immune-resistant tumor model (P3), thereby developing a system that would allow us to identify genes that may contribute to tumor escape from vaccine-mediated immune responses.⁵

On the basis of this model, we have employed a novel strategy to identify molecules involved in tumor immune evasion. Since downregulation of MHC class I molecules is a common mechanism of tumor immune evasion, we generated subclones of the immunoresistant P3 tumors and characterized the MHC class I expression profile of these clones compared to P0 and P3 tumors. While the majority of subclones from P3 tumors demonstrated decreased MHC class I expression compared to the parental TC-1/P0 tumors, one particular subclone, A17, demonstrated comparable level of MHC class I expression compared to TC-1/P0 tumors, suggesting other mechanisms that may contribute to immune escape.

In this study, we observed that the immune-resistant subclone, A17 was resistant to apoptotic cell death induced by E7-specific CD8⁺ T cells *in vitro* and *in vivo*. The A17 tumor cells demonstrated upregulation of several antiapoptotic proteins, which was mediated by Akt activation, thus resulting in the immune resistance phenotype of A17 tumors. In addition, Akt inhibition was capable of reversing the immune-resistant phenotype of tumors, rendering them susceptible to effective immunotherapy. Thus, we have successfully identified Akt activation as an innovative mechanism for tumor immune evasion. The clinical implications of the current study are discussed.

RESULTS

Immunoresistant A17 tumor cells demonstrate comparable levels of E7 expression and the ability to activate E7-specific CD8⁺ T cells compared to TC-1 tumors

Using the immunoresistant P3 tumor model, we generated various P3 subclones; A1 to A20. We determined the surface MHC class I expression of P0 and P3 tumors. We found that the majority of subclones of P3 tumors have low levels of MHC class I expression compared to P0/TC-1 tumors. However, three subclones including A3, A9 and A17 demonstrated comparable level of MHC class I expression compared to TC-1/P0 tumors (**Supplementary Figure S1**). Among the three subclones, A17 showed quite similar MHC class I expression levels as TC-1/P0 tumors. Therefore, we further evaluated the phenotypic and functional characteristics of the A17 tumor cells. As shown in **Figure 1a**, we observed that A17 tumor cells demonstrated comparable expression levels of MHC class I compared to the TC-1/P0 cells. The A17 and TC-1/P0 tumor cells also showed comparable expression levels of E7 (**Figure 1b**). We also sequenced the HPV-16 E7 gene within the A17 tumor cells and found no mutations (data not shown), thus precluding the alteration of the immunodominant epitope of E7. Furthermore, to determine the ability of A17 to process and present the E7 peptide through the MHC class I pathway, we characterized the ability of A17 tumor cells to activate E7-specific CD8⁺ T cells compared to TC-1/P0 tumors. As shown in **Figure 1c**, we observed that A17 tumor cells demonstrated a comparable ability

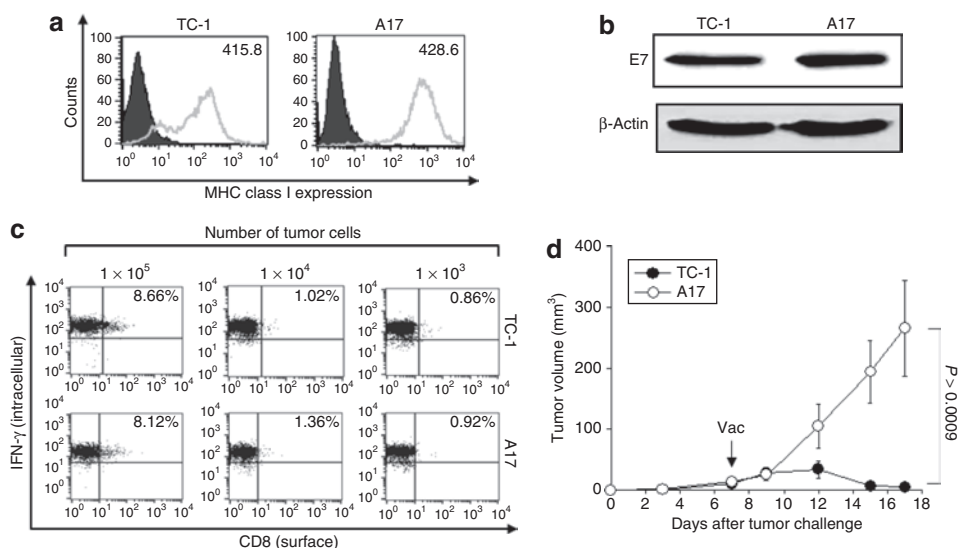


Figure 1 Phenotypical and functional characterization of A17 tumor cells. **(a)** Flow cytometry analysis to characterize MHC class I expressions on TC-1 and A17 tumor cells. PE-conjugated antimouse H-2D^b monoclonal antibody was used to detect MHC class I expression. The isotype antibody was used as the negative control (gray profile). **(b)** Western blot analysis to characterize the expression of E7 in the TC-1 and A17 tumor cells. Equal amounts of cell lysates (50 μ g) from TC-1 and A17 tumor cells were loaded and separated by sodium dodecyl sulphate–polyacrylamide gel electrophoresis using a 15% polyacrylamide gel. After electroblotting, the membranes were probed with E7-specific antibody, and then incubated with goat antimouse IgG conjugated to horseradish peroxidase for visualization of E7 protein using Hyperfilm-enhanced chemiluminescence. **(c)** Intracellular cytokine staining and flow cytometry analysis to determine the number of IFN- γ secreting E7-specific CD8⁺ T cells induced by TC-1 and A17 tumor cells. TC-1 and A17 tumor cells were incubated with E7-specific CD8⁺ T cells at 0.01:1, 0.1:1, and 1:1 ratio of tumor cells:T cells for 16 hours. After incubation, cells were stained for CD8⁺ and IFN- γ , and were subjected to flow cytometry analysis to detect activated E7-specific CD8⁺ T cells. Data shown are representative of three independent experiments. **(d)** C57BL/6 mice (five per group) were inoculated subcutaneously with 1×10^5 /mouse of TC-1 or A17 tumor cells. Five days after tumor challenge, mice were treated with Vac-Sig/E7/LAMP-1. Tumor volumes (mm^3) from TC-1 and A17 groups were recorded twice per week for 18 days following immunization. Tumor treatment experiments were performed three times to generate reproducible data.

to activate E7-specific CD8⁺ T cells *in vitro* compared to TC-1/P0 tumors. This result suggests that the antigen processing and presentation of E7 through the MHC class I was not impaired in A17 tumors relative to TC-1/P0 tumors.

We further determined whether the A17 tumor cells were immune resistant similar to the parental P3 tumors. C57BL/6 mice (five per group) were inoculated subcutaneously with 1×10^5 /mouse of TC-1/P0 or A17 tumor cells. Five days after tumor challenge, mice were treated with Vac-Sig/E7/LAMP-1. Tumor volumes were recorded twice per week for 18 days following immunization. As shown in **Figure 1d**, A17 tumor-challenged mice showed significantly higher tumor volumes over time compared to TC-1 tumor-challenged mice, thus demonstrating immune resistance. This indicates that the A17 tumor cell line is

immune resistant. Taken together, our data suggest that although A17 tumor cells express high levels of MHC class I, demonstrate comparable levels of E7 expression and an ability to activate E7-specific CD8⁺ T cells, they maintain the immune resistance of the parental P3 tumor cell line.

A17 tumors are resistant to apoptotic cell death induced by E7-specific CD8⁺ T cells *in vitro* and *in vivo*

To determine whether the immune resistance of A17 tumor cells is related to the apoptotic cell death induced by cytotoxic T-lymphocyte (CTL) killing, TC-1/P0 and A17 tumor cells were incubated with E7-specific CD8⁺ T cells at different effector:target (E:T) ratios (1:1, 0.5:1, or 0.1:1) for 4 hours and the percentage of apoptotic cells was analyzed using flow cytometry for active caspase-3 expression. As shown in **Figure 2a**, there was a significantly lower percentage of apoptotic A17 tumor cells compared to apoptotic TC-1/P0 tumor cells at different E:T ratios compared to TC-1/P0 tumors. A graphical representation of the percentage of apoptotic tumor cells at different E:T ratios is depicted in **Figure 2b**. We further characterized the number of viable TC-1/P0 and A17 tumor cells which were incubated with E7-specific CD8⁺ T cells at 1:1 ratio of tumor:T cells for 16 hours by staining with Trypan blue. As shown in **Figure 2c**, the number of viable tumor cells was significantly higher in the A17 tumors compared to the TC-1 tumors. This observation was also confirmed by direct observation of the cell morphology of TC-1 and A17 tumor cells using light microscopy after incubation with E7-specific CD8⁺ T cells overnight.

To assess the immune resistance of the tumor cell lines to the apoptotic cell death induced by adoptively transferred E7-specific CD8⁺ T cells *in vivo*, C57BL/6 mice (five per group) were challenged subcutaneously with TC-1 or A17 tumor cells. Seven days after tumor challenge, mice were adoptively transferred E7-specific CD8⁺ T cells intravenously through the tail vein. Mice were monitored twice a week for tumor growth. As shown in **Figure 2d**, TC-1 tumor-challenged mice treated with E7-specific CD8⁺ T cells demonstrated significantly lower tumor volume over time compared to A17 tumor-challenged mice treated with E7-specific CD8⁺ T cells. In contrast, there was no significant difference in the tumor volumes of untreated TC-1 or A17 tumor-challenged mice. Thus, our data indicate that A17 tumor cells are highly resistant to apoptotic cell death induced by E7-specific CD8⁺ T cells *in vitro* as well as *in vivo*.

Akt activation plays a role in the resistance of A17 apoptotic tumor cell death induced by E7-specific CD8⁺ T cells

To characterize the expression of the various key anti- and proapoptotic proteins expressed by the A17 and TC-1/P0 tumor cells, we performed western blot analysis using A17 and TC-1/P0 tumor cell lysates. As shown in **Figure 3a**, the expression of the antiapoptotic proteins including Bcl-2, Bcl-xL, phosphorylated Bad (p-Bad), Bcl-w, cIAP-2, and survivin was significantly increased in the A17 tumor cells compared to TC-1/P0 tumor cells. In comparison, the expression of key proapoptotic proteins including Bak, Bax, Bad, Bim, and Bid was not significantly different between A17 cells and TC-1/P0 cells. Thus, our results suggest the global upregulation of antiapoptotic proteins.

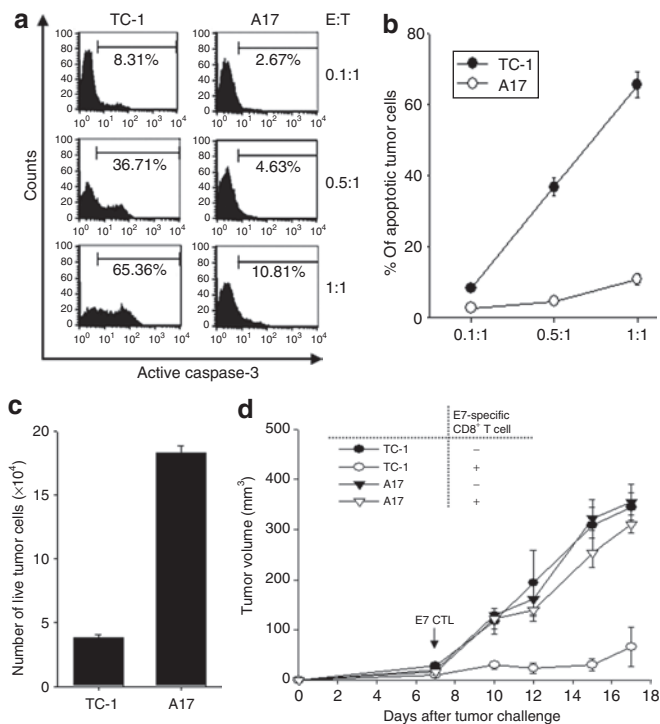


Figure 2 Characterization of apoptotic cell death of the TC-1 and A17 tumors induced by E7-specific CD8⁺ T cells *in vitro* and *in vivo*. **(a)** Flow cytometry analysis to characterize active caspase-3 expression in TC-1 and A17 tumor cells induced by E7-specific CD8⁺ T cells. TC-1 and A17 tumor cells were incubated with E7-specific CD8⁺ T cells at different E:T ratios (1:1, 0.5:1 or 0.1:1) for 4 hours. Detection of apoptotic cells in the TC-1 and A17 tumor cells was performed using PE-conjugated rabbit anti active caspase-3 antibody. The percent of apoptotic cells was analyzed using flow cytometry for active caspase-3 expression. Data shown are representative of three independent experiments. **(b)** Graphical representation of the percentage of apoptotic TC-1 and A17 tumor cells at different E:T ratios. **(c)** Bar graph depicting number of viable TC-1 and A17 tumor cells. TC-1 and A17 tumor cells were incubated with an E7-specific CD8⁺ T-cell line at 1:1 ratio of tumor:T cells for 16 hours. The number of viable tumor cells was determined using Trypan blue staining (mean \pm SD). **(d)** Graphical representation of the tumor volume in mice challenged with TC-1 or A17 tumor cells with or without adoptive transfer of E7-specific CD8⁺ T cells. C57BL/6 mice (five per group) were challenged subcutaneously with 1×10^5 /mouse of TC-1 and A17 tumor cells in the left leg. Seven days after tumor challenge, mice received 2×10^6 /mouse of E7-specific CD8⁺ T cells intravenously via tail vein. Mice were monitored twice a week for tumor growth. Tumor treatment experiments were performed three times to generate reproducible data.

We then performed western blot analysis to determine the expression of the various signaling molecules that may play a role in the global control of apoptosis. We analyzed the expression of total Akt, Ser 473 phosphorylated pAkt, total Erk, Thr 202/Tyr 204 phosphorylated pErk, total p38 MAP kinase and Thr 180/Tyr 182 phosphorylated pp38 MAP kinase. We observed that the expression of pAkt was significantly increased in the A17 tumor cells compared to TC-1/P0 as compared to all of the apoptotic proteins characterized (Figure 3b). Interestingly, no difference was observed in the expression of Akt in the TC-1/P0 and A17 tumors. Thus, our data indicate that Akt activation plays a role in the immune resistance of A17 tumor cells against apoptotic tumor cell death induced by E7-specific CD8⁺ T cells.

Activation of Akt in TC-1/P0 cells induces an immune resistance phenotype *in vitro* and *in vivo*

To determine whether activation of Akt in TC-1/P0 cells results in an immune resistance phenotype, we transfected TC-1/P0 cells with a DNA construct encoding HA-tagged myristylated Akt (myrAkt) (TC-1/CA-Akt). Because myrAkt has a myristoylation signal at its N terminus, the protein is not only constitutively localized to the plasma membrane but also maintains a constitutively active status in the cell.^{6,7} TC-1/P0 cells transfected with no insert (pMSCV) were used as a control (TC-1/no insert). We performed a western blot with these constructs to characterize the expression of Akt, pAkt and HA. As shown in Figure 4a, the TC-1/CA-Akt tumor cells expressed pAkt and HA compared to the TC-1/no insert. We further characterized the expression of the various key anti- and proapoptotic proteins in these two tumor cell lines. We found that the expression of antiapoptotic proteins (Bcl-2, Bcl-xL, p-Bad, Bcl-w, cIAP-2, survivin) was significantly increased in the TC-1/CA-Akt tumor

cells compared to the TC-1/no insert cells. In comparison, the expression of key proapoptotic proteins (Bak, Bax, Bad, Bim, Bid) was decreased in TC-1/CA-Akt cells compared to TC-1/no insert cells (Figure 4b). We then performed flow cytometry analysis to compare the resistance to CTL-induced apoptosis *in vitro* between the TC-1/No insert and TC-1/CA-Akt tumor cells. For this, TC-1/No insert and TC-1/CA-Akt tumor cells were incubated with E7-specific CD8⁺ T cells at different E:T ratios (1:1, 0.5:1 or 0.1:1) for 4 hours. The percentage of apoptotic cells was analyzed using flow cytometry for active caspase-3 expression. As shown in Figure 4c, there was a significantly lower percentage of apoptotic cells in the TC-1/CA-Akt tumor cells compared to the TC-1/no insert cells.

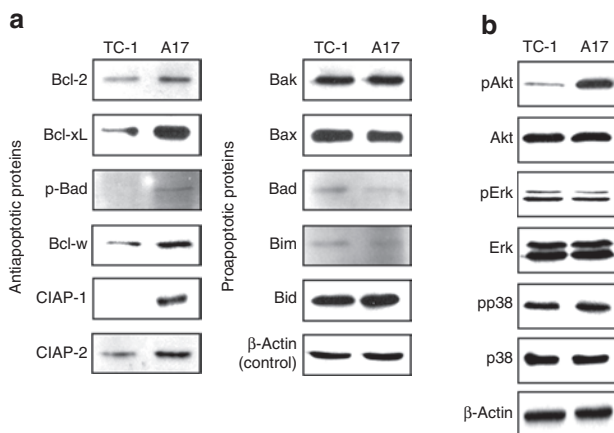


Figure 3 Akt activation contributes to the resistance of A17 apoptotic tumor cell death induced by E7-specific CD8⁺ T cells. Equal amounts of cell lysates (50 μg) from TC-1 and A17 tumor cells were loaded and separated by sodium dodecyl sulphate–polyacrylamide gel electrophoresis using 10% polyacrylamide gel. β-Actin was used as a loading control. (a) Western blot analysis to characterize the expression of various key antiapoptotic proteins including Bcl-2, Bcl-xL, p-Bad, Bcl-w, cIAP-2, survivin and key pro apoptotic proteins including Bak, Bax, Bad, Bim, Bid in the TC-1 and A17 tumor cells. (b) Western blot analysis to characterize the expression of total Akt, Ser 473 pAkt, total Erk, Thr 202/Tyr 204 pErk, total p38 MAP kinase and Thr 180/Tyr 182 pp38 MAP kinase in the TC-1 and A17 tumor cells.

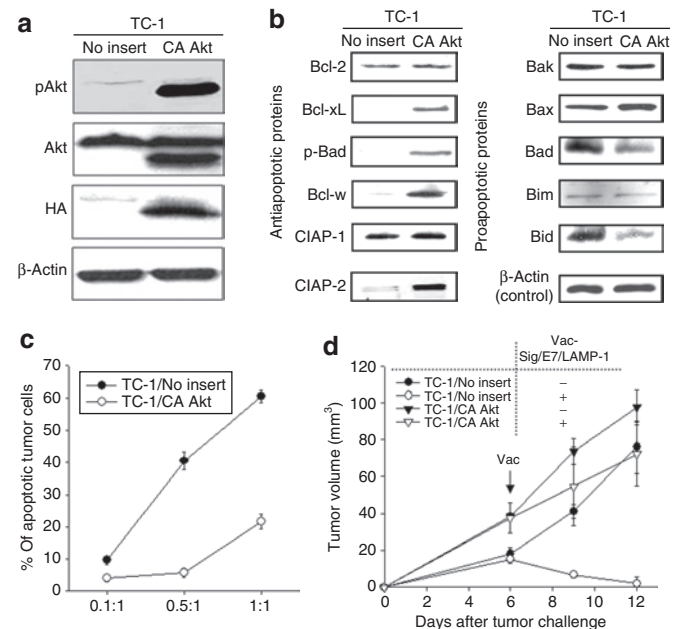


Figure 4 Characterization of apoptotic cell death of TC-1/no insert and TC-1/CA Akt cells induced by E7-specific CD8⁺ T cells *in vitro* and *in vivo*. (a,b) Equal amounts of cell lysates (50 μg) from TC-1/No insert and TC-1/CA Akt tumor cells were loaded and separated by sodium dodecyl sulphate–polyacrylamide gel electrophoresis using 10% polyacrylamide gel. β-Actin was used as a loading control. (a) Western blot analysis to characterize the expression of total Akt, Ser 473 pAkt, and hemagglutinin (HA) in the TC-1/No insert and TC-1/CA Akt tumor cells. (b) Western blot analysis to characterize the expression of key antiapoptotic proteins including Bcl-2, Bcl-xL, p-Bad, Bcl-w, cIAP-2, survivin and key pro apoptotic proteins including Bak, Bax, Bad, Bim, Bid in the TC-1/No insert and TC-1/CA Akt tumor cells. (c) Graphical representation of the percentage of apoptotic TC-1/no insert or TC-1/CA Akt tumor cells at different E:T ratios (1:1, 0.5:1 or 0.1:1) for 4 hours. Detection of apoptotic cells in the TC-1/No insert and TC-1/CA Akt tumor cells was performed using PE-conjugated rabbit anti active caspase-3 antibody. The percentage of apoptotic cells was analyzed using flow cytometry for active caspase-3 expression. Data shown are representative of three independent experiments. (d) Graphical representation of the tumor volume in mice challenged with TC-1/No insert and TC-1/CA Akt tumor cells with or without vaccination with Vac-Sig/E7/LAMP-1. C57BL/6 mice (five per group) were inoculated subcutaneously with 1 × 10⁵/mouse of TC-1/No insert and TC-1/CA Akt cells. Five days after tumor challenge, mice were treated with Vac-Sig/E7/LAMP-1. Tumor volumes (mm³) from TC-1/No insert and TC-1/CA Akt groups were recorded twice per week for 7 days following immunization. Tumor treatment experiments were performed three times to generate reproducible data.

We further assessed resistance of the TC-1/CA-Akt tumor cells to apoptotic tumor cell death induced by E7-specific CD8⁺ T cells *in vivo*. C57BL/6 mice (five per group) were challenged subcutaneously with TC-1/no insert or TC-1/CA-Akt tumor cells. Seven days after tumor challenge, mice received either Vac-Sig/E7/LAMP-1 vaccination or E7-specific CD8⁺ T cells intravenously through the tail vein. Mice were monitored twice a week for tumor growth. TC-1/no insert tumor-challenged mice treated with either Vac-Sig/E7/LAMP-1 (Figure 4d) or E7-specific CD8⁺ T cells (Supplementary Figure S2) demonstrated significantly lower tumor volume over time compared to TC-1/CA Akt tumor-challenged mice treated with either Vac-Sig/E7/LAMP-1 or E7-specific CD8⁺ T cells. In contrast, there was no significant difference in the tumor volumes of untreated TC-1/no insert or TC-1/CA-Akt tumor-challenged mice. Thus, taken together, our data indicate that TC-1/CA-Akt tumor cells are resistant to apoptotic tumor cell death induced by E7-specific CD8⁺ T cells *in vitro* as well as *in vivo*.

Treatment of A17 tumor cells with the Akt inhibitor, API-2, reduces the expression of antiapoptotic proteins resulting in an increase in the apoptosis of tumor cells

To confirm the role of Akt in the resistance of A17 apoptotic tumor cell death induced by E7-specific CD8⁺ T cells, we employed a pharmacological inhibitor of Akt, Akt/protein kinase B signaling inhibitor-2 (API-2).⁸ API-2 has been shown to suppress the kinase activity and phosphorylation level of Akt leading to inhibition of cell growth and induction of apoptosis.⁸ As shown in Figure 5a,

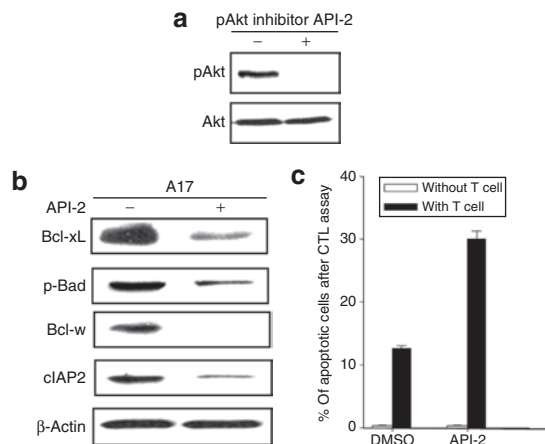


Figure 5 Characterization of the expression of antiapoptotic proteins and percentage of apoptosis after treatment with the Akt inhibitor, API-1. (a) Western blot analysis to characterize the level of total Akt and Ser 473 pAkt in the A17 tumor cells in the presence or absence of API-1. A17 tumor cells were incubated with the pharmacological pAkt inhibitor API-2 for 24 hours prior to lysate preparation. Blots are representative of three separate experiments. (b) Western blot analysis to characterize the expression of the key antiapoptotic proteins in the presence and absence of API-2 inhibitor. A17 tumor cell was incubated with API-2 (10 nmol/l) for 24 hours prior to lysate preparations. β-Actin was used as a loading control. (c) Graphical representation of the percentage of apoptotic A17 tumor cells in the presence or absence of E7-specific CD8⁺ T cells. A17 tumor cells were pretreated with dimethyl sulfoxide (DMSO) or API-2 and incubated with an E7-specific CD8⁺ T cell at E:T ratios 0.5:1 for 4 hours. After incubation, cells were stained using PE-conjugated rabbit anti active caspase-3 antibody.

we demonstrated successful inhibition of pAkt using the inhibitor API-2. We then characterized the influence of the API-2 inhibitor in the expression of key antiapoptotic proteins in A17 tumor cells. As shown in Figure 5b, the expression of the antiapoptotic proteins (Bcl-xL, p-Bad, Bcl-w, cIAP-2) in the A17 tumor cells was significantly reduced in the presence of the pAkt inhibitor, API-2. Furthermore, the A17 tumor cells treated with the API-2 inhibitor demonstrated increased susceptibility to apoptotic cell death induced by E7-specific CD8⁺ T cells (Figure 5c). Thus, our data indicate that treatment with the Akt inhibitor, API-2, reduces the expression of antiapoptotic proteins and results in increased apoptosis of A17 tumor cells, confirming the role of Akt in the resistance of A17 apoptotic tumor cell death induced by E7-specific CD8⁺ T cells.

Treatment with the Akt inhibitor reverses the immune-resistant phenotype of A17 tumors and renders them susceptible to effective immunotherapy

To determine whether the combination of immunotherapy using vaccination or adoptive T-cell transfer with Akt inhibitor treatment can enhance the antitumor effects against A17 tumor cells, C57BL/6 mice (three per group) were inoculated subcutaneously with 1×10^5 A17 tumor cells per mouse. Seven days after tumor challenge, mice were immunized with either Vac-Sig/E7/LAMP-1 or Vac-WT. Another group of A17 tumor-challenged mice were treated either with adoptively transferred E7-specific CD8⁺ T cells or normal saline. Three days later, all the mice were intratumorally injected with API-2. Tumor volumes were recorded twice per week for 10 days following immunization. As shown in Figure 6a, tumor-challenged mice treated with Vac-Sig/E7/LAMP-1 combined with API-2 treatment demonstrated significantly lower tumor volume over time compared to tumor-challenged mice treated with Vac-WT combined with API-2. A graphical representation of the tumor weights and representative images of the tumor are depicted in Figure 6b. Furthermore, tumor-challenged mice treated with adoptively transferred E7-specific CD8⁺ T cells combined with API-2 treatment demonstrated significantly lower tumor volume over time compared to tumor-challenged mice treated with API-2 and normal saline (Figure 6c). A graphical representation of the tumor weights and representative images of the tumors are depicted in Figure 6d. We also observed that inhibition of Akt rendered human cancer cells sensitive to CTL-induced apoptosis *in vitro* and *in vivo* (Supplementary Figure S3). Thus, taken together, our data suggest that Akt inhibition is capable of reversing the immune-resistant phenotype of different tumors, rendering them susceptible to effective immunotherapy.

DISCUSSION

In this study, we used a novel approach to identify the pathways involved in tumor immune evasion. We identified a particular subclone of immune-resistant P3 tumors (A17) that expressed comparable levels of MHC class I compared to TC-1/P0 tumors yet were resistant to apoptotic cell death induced by E7-specific CD8⁺ T cells *in vitro* and *in vivo*. The A17 tumor cells demonstrated upregulation of several antiapoptotic proteins, which was mediated by Akt activation, thus resulting in the immune resistance phenotype of A17 tumors. In addition, Akt inhibition was

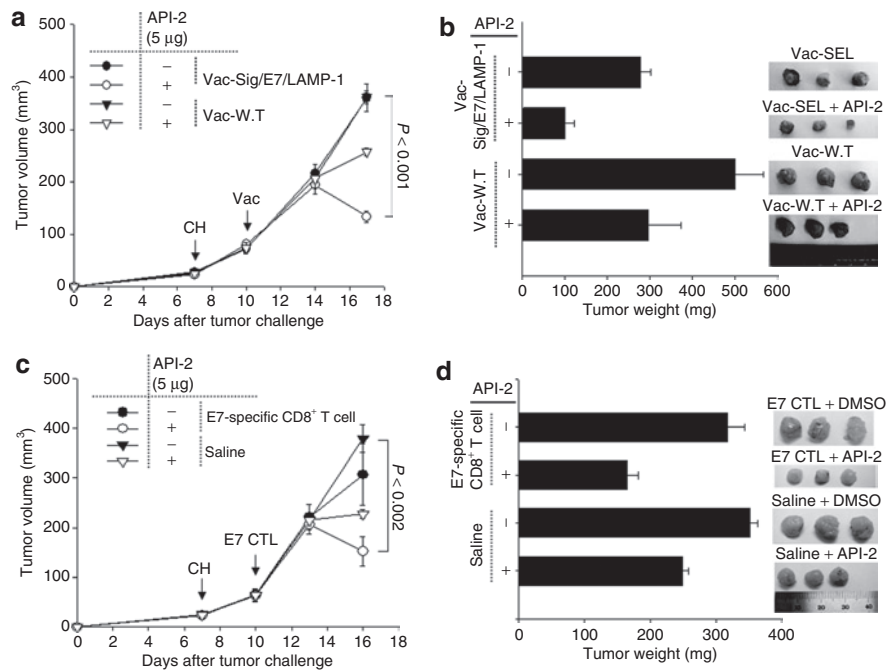


Figure 6 Characterization of antitumor effects generated by Vac-Sig/E7/LAMP-1 vaccination or E7-specific CD8⁺ T-cell adoptive transfer combined with Akt inhibitor (API-2) treatment. C57BL/6 mice (three per group) were inoculated subcutaneously with 1×10^5 /mouse of A17 tumor cells. Seven days after tumor challenge, **(a,b)** one set of mice were immunized with 1×10^7 pfu/mouse of Vac-Sig/E7/LAMP-1 while **(c,d)** another set of mice were treated with 2×10^6 /mouse of adoptively transferred E7-specific CD8⁺ T cells. Three days after immunization, mice were injected intratumorally with chitosan hydrogel containing 5 μ g API-2. **(a,c)** Tumor volumes from A17 tumor was recorded twice per week for 10 days following immunization. Line graph representing the tumor volume of A17 tumor-challenged mice treated with API-2 and **(a)** with or without the DNA vaccination or **(c)** in the presence or absence of E7-specific CD8⁺ T cells. **(b,d)** Bar graph and representative images representing tumor weights and morphology from challenged mice treated with API-2 and **(b)** with or without the DNA vaccination or **(d)** in the presence or absence of E7-specific CD8⁺ T cells on 17 days after tumor challenge.

capable of reversing the immune-resistant phenotype of tumors, rendering them susceptible to effective immunotherapy. Thus, our study identifies activation of the Akt pathway as a mechanism for tumor immune escape.

Expression of the active form of Akt has been shown to contribute to the resistance of tumor cells to chemotherapy^{8,9} and/or radiation therapy.¹⁰ In this study, we also observed that A17 tumors demonstrate resistance to chemotherapy and radiation compared to P0 tumors (data not shown). Furthermore, inhibition of Akt was able to render the A17 tumor cells more susceptible to chemotherapy and radiation (see **Supplementary Figure S4**). Thus, our study is consistent with previous results, showing that expression of active Akt in A17 tumor cells enhances tumor resistance to chemotherapy and radiation therapy. Furthermore, Akt signaling has been shown to mediate resistance against tumor suppression by antigen-specific T cells *in vitro* and adoptively transferred cellular immune effectors *in vivo*.¹¹ Taken together, these data suggest that resistance to various cancer therapeutic agents including tumor-specific CD8⁺ T-cell immune response may be related to the Akt signaling pathway. Thus, the evasion of apoptotic cell death induced by T cells or conventional cancer killing agents may be considered a hallmark of multi-resistance to cancer therapy.

The identification of expression of the active form of Akt as a mechanism for tumor immune evasion has significant clinical implications. Several clinical trials have demonstrated that the successful generation of tumor-specific immune responses

in vaccinated patients did not necessarily correlate with tumor regression in cancer patients (for review, see ref. 1). We have also observed similar findings in patients with HPV-16 associated high-grade cervical intraepithelial neoplasia lesions who were vaccinated with an HPV-16 E7 therapeutic DNA vaccine. We observed that in some vaccinated patients appreciable levels of HPV-16 E7-specific CD8⁺ T-cell immune responses were generated which correlated with lesion regression; however, in some patients failed to demonstrate lesion regression in spite of generating appreciable levels of E7-specific immune responses (T.-C. Wu, unpublished results). Thus, it would be of interest to characterize the expression levels of the active form of Akt in these clinical specimens. The demonstration of upregulation of Akt in the clinical specimens from patients who failed to show lesion regression would confirm that the active form of Akt plays an important role in immune evasion.

We also observed that API-2 treatment reverses the immune-resistant phenotype of A17 tumors and renders them susceptible to effective immunotherapy. This finding has immense clinical relevance since the Akt inhibitor; API-2, has been widely used in several clinical trials. API-2 is a synthetic small molecule compound, which was previously identified as tricyclic nucleoside. A number of phase I and II clinical trials using API-2 have been conducted in patients with advanced tumors, including carcinomas of the pancreas, lung, breast, colon, bladder, and ovary (for review see ref. 12). Thus, it is conceivable that API-2 can be used in conjunction with immunotherapy to result in better therapeutic effects in the clinical arena.

We also observed that treatment with API-2 alone can itself generate appreciable antitumor effects against A17 tumors (see **Figure 6**). Since the Akt pathway plays a pivotal role in malignant transformation by inducing cell survival, growth, migration, and angiogenesis, the inhibition of Akt using API-2 may potentially play a role in suppression of cell growth and induction of apoptosis in human cancer cells that express Akt. Indeed, studies have shown that API-2 potently inhibits tumor growth in human cancer cells in which Akt is aberrantly expressed/activated.⁸ Thus, the employment of API-2 may potentially contribute to the antitumor effect independent of therapeutic vaccines.

In our study we have monitored the tumor size in tumor bearing mice treated with Vac-Sig/E7/LAMP-1 or adoptive T-cell transfer combined with or without API-2 treatment twice per week for 10 days following immunization. However, the duration for follow-up of the tumor growth is limited by the release of API-2 from the chitosan hydrogel (CH). We observed a more obvious difference in the antitumor effect starting from day 14 and peaks at day 16 (see **Figure 6**). However, the difference in the antitumor effects among different groups gradually disappears by day 23 (data not shown). In our previous study, we have demonstrated that CH system used in this study was completely degraded and disappeared 7 days after injection under our experimental conditions.¹³ Thus, the follow-up of tumor growth after tumor challenge and treatment is quite limited in this case. Nevertheless, our data suggest that Akt inhibitor treatment can significantly enhance the therapeutic efficacy of tumor antigen-specific T-cell immune responses against the immune-resistant tumors.

In summary, we have identified that upregulation of the active form of Akt is an innovative mechanism of tumor immune evasion. In addition, we have demonstrated that inhibition of Akt using API-2 can render human cancer cells that upregulate pAkt susceptible to effective immunotherapy. Thus, our findings have immense potential for future clinical translation using Akt inhibitors in combination with immunotherapy for the control of cancer.

MATERIALS AND METHODS

Mice. Six- to 8-week-old female C57BL/6 mice and the nude mice were purchased from Daehan Biolink (Chungbuk, Korea). All animal procedures were done in accordance with recommendations for the proper use and care of laboratory animals.

DNA constructs. For the generation of the pMSCV/CA Akt construct, the DNA fragment encoding HA-tagged CA-Akt Δ 4-129, which contains a *src* myristoylation signal sequence was amplified from pECE-myrAkt, (a kind gift from Dr Jongkyeong Chung, KAIST; Daejeon, Korea)¹⁴ using a set of primers: 5'-GGAGATCTACCATGGGGAGTAGCAAGAGCAAG-3' and 5'-GGCTCGAGTCACAGTCCAGGTCCCAGAC-3'. The amplified DNA was subsequently cloned into the Bgl II/Xho I sites of pMSCV retroviral vector (Clontech, Mountain View, CA).

For the generation of pMSCV/SCT E7 construct, DNA fragment encoding the immunodominant E7 aa 49-57 peptide and flanking *AgeI/NheI* restriction enzyme sites was made by annealing two single-stranded oligo-nucleotides 5'-CCGG AGA GCC CAT TAC AAT ATT GTA ACC TTT-3' and 5'-CTAG TCT CGG GTA ATG TTA TAA CAT TGG AAA-3'. It was then cloned into pIRES-E6-K^b (ref. 15) using *AgeI/NheI* sites to replace the E6 epitope, generating pIRES-E7-2m-K^b. E7-2m was then amplified with PCR using pIRES-E7-2m-K^b as the

template and a set of primers, 5'-AGA TCT AGA GCC CAT TAC AAT ATT GTA ACC TTT-3' and 5'-CTC GAG GGT GGT GGA GGT AGT GGC GGG GCG ATG GCT CCG CGC ACG CTG C-3'. The amplified product was then cloned into the BglII/XhoI sites of pMSCV/D^b vector, which was inserted with PCR-amplified D^b gene using cDNA library from a dendritic cell line, DC2.4, as the template and a set of primers 5'-CTC GAG ATC CGG TGG TGG AGG TAG TGG CCC ACA CTC GAT GCG GTA TT-3' and 5'-GAA TTC AAC AAT TGT CAC GCT TTA CAA TCT CGG AGA G-3' into XhoI/EcoRI sites of pMSCV (Clontech, CA). Plasmid constructs were confirmed by DNA sequencing.

Reagents and cell lines. The drug, API-2 (Calbiochem, San Diego, CA) was used for inhibition of the Akt pathway. Four HPV-16 E7-expressing cell lines, TC-1, TC-1 P3 (A17), TC-1/No insert, and TC-1/CA Akt, were used as murine tumor models. The production and maintenance of TC-1 cells has been described previously.² A17 was generated from TC-1 P3 clones, outgrowth tumors from vaccinated mice *in vivo*, which has been previously described.⁵ Among the TC-1 P3 clones, a representative clone with normal level of MHC class I expression was isolated, expanded, and designated as the TC-1 P3 (A17) tumor cell line.

For the generation of TC-1/CA Akt cell line, the constructed pMSCV/CA Akt or pMSCV/No insert DNAs were transfected into the Phoenix packaging cell line, and the virus-containing supernatant was collected 48 hours after transfection. The supernatant was immediately concentrated using a Centrifugal filter devices (Millipore, Bedford, MA) and used to infect target cells (TC-1) in the presence of 8 μ g/ml polyethylenimine (Sigma, St Louis, MO). One day after retroviral transduction, the virus supernatant was replaced with normal culture medium, and when the cells reached 70% confluency, puro mycin (5 μ g/ml) was used to select for cells with integrated pMSCV/CA Akt. Four cell lines (TC-1, A17, TC-1/No insert, and TC-1/CA Akt) were cultured in RPMI 1640 medium containing 2mmol/l L-glutamine, 1mmol/l sodium pyruvate, nonessential amino acid, 100IU penicillin/streptomycin and 10% fetal bovine serum in a 37°C incubator with 5% CO₂.

The CaSki/SCT E7 is a CaSki cell line expressing single-chain trimer of MHC class I (H-2D^b) linked to an HPV-16 E7 immunodominant CTL epitope (aa 49-57), which can be recognized and killed by an HPV-16 E7-specific CD8⁺ T-cell line.¹⁶ For the generation of the CaSki/SCT E7 cell line, the constructed pMSCV/SCT E7 was transfected into the Phoenix packaging cell line for collecting the virus-containing supernatant. One day after retroviral transduction of CaSki with the virus supernatant, the transduced CaSki/SCT E7 cells were selected using puromycin (5 μ g/ml) as described above. The CCD-1120Sk (ATCC number: CRL-2510), a fibroblast cell line established from a human skin taken from normal tissue, was used as a normal epithelial cell for comparison of Akt activation.

Generation of E7-specific T-cell line. The generation of the E7-specific T-cell line has been described previously.¹⁶ Briefly, C57BL/6 (H-2b) mice were immunized using intraperitoneal injection of 10⁷ pfu. of Sig/E7/LAMP-1 vaccinia virus. Splenocytes were harvested at day 8 after immunization. Autologous, irradiated splenocytes pulsed with 1 μ g/ml of E7 peptide (amino acid 49-57) were used as stimulators. Recombinant human IL-2 was added to the culture at a final concentration of 30 U/ml. The specificity of the E7-specific T-cell line was confirmed by IFN- γ ELISPOT assay following stimulation with E7-specific peptide (aa 49-57).¹⁶

Flow cytometry analysis. For *in vitro* E7-specific CD8⁺ T-cell activation, TC-1 and A17 tumor cells were incubated with an E7-specific CD8⁺ T-cell line at 0.01:1, 0.1:1, and 1:1 ratio of tumor:T cells for 16 hours. Cell surface marker staining of CD8 and intracellular cytokine staining for IFN- γ as well as FACSscan analysis was performed using conditions described previously.¹⁷⁻²⁰ To detect MHC class I expression, PE-labeled antimouse H-2K^b or H-2D^b (BD Biosciences, San Diego, CA) monoclonal antibody was used. After incubation with primary antibody, cells were washed with

phosphate-buffered saline. Analysis was done on a Becton Dickinson FACSscan with CELLQuest software (BD Biosciences).

CTL-mediated cytotoxicity. For the *in vitro* CTL assay, TC-1, A17, TC-1/No insert and TC-1/CA-Akt tumor cells were harvested by trypsinization, and washed once with RPMI (Hyclone, Logan) containing 0.1% fetal bovine serum and resuspended in 1 ml of RPMI containing 0.1% fetal bovine serum. Cells were incubated for 10 minute with 10 μ mol/ml of carboxyfluorescein succinimidyl ester (CFSE). CFSE-labeled TC-1, A17, TC-1/No insert and TC-1/CA Akt were incubated for 4 hours with E7-specific CD8⁺ T-cell line at various E:T ratios (1:1, 0.5:1, or 0.1:1) at 37°C with 5% CO₂. To detect apoptotic cells, cells were then labeled with PE-conjugated antiactive caspase-3 antibody (BD Bioscience, San Diego, CA) according to manufacturer's instructions. The percentage of apoptotic tumor cells was analyzed using flow cytometry analysis by gating CFSE⁺ and active caspase-3⁺ cells. The number of live tumor cells were also determined after overnight incubation with 1 \times 10⁵ E7-specific CD8⁺ T cells at the various E:T ratios using 0.4% Trypan blue. The cells were counted using a hemacytometer and light microscopy.

For the *in vitro* CTL assay, CFSE-labeled CaSki/SCT E7 tumor cells were pretreated with dimethyl sulfoxide or API-2 for 24 hours, and then incubated with an E7-specific CD8⁺ T-cell line¹⁶ at different E:T ratios (1:1, 5:1 or 10:1) for 4 hours. The percentage of apoptotic cells in CFSE⁺ CaSki/SCT E7 tumor cells were measured by flow cytometry using a PE-conjugated rabbit antiactive caspase-3 antibody.

In vivo tumor treatment experiments. For the *in vivo* tumor treatment experiments, on the day of tumor challenge, tumor cells were harvested by trypsinization, washed once with Opti-MEM I (Gibco) and resuspended in 1 ml of Opti-MEM I to the designated concentration for subcutaneous injection. Mice were subcutaneously challenged with 1 \times 10⁵ TC-1, TC-1 P3 (A17), TC-1/No insert or TC-1/CA-Akt tumor cells per mouse in the left leg. Seven days after tumor challenge, one set of mice were immunized with 1 \times 10⁷ pfu/mouse of Vac-Sig/E7/LAMP-1 while another set of mice were treated with 2 \times 10⁶ mouse of adoptively transferred E7-specific CD8⁺ T cells intravenously through the tail vein.¹⁶ For the Sig/E7/LAMP-1 vaccinia virus vaccination, the virus was thawed, trypsinized with trypsin/EDTA in 37°C water bath for 30 min, and diluted with Opti-MEM I to the final concentration of 1 \times 10⁸ PFUs/ml. Seven days after tumor challenge, 1 \times 10⁷ PFUs of Sig/E7/LAMP-1 vaccinia virus were injected intraperitoneally into C57BL/6 mice. Three days after immunization, mice were injected intratumorally with CH containing 5 μ g API-2. Tumor volumes from A17 tumor was recorded twice per week for 10 days following immunization.

For the *in vivo* tumor treatment experiments using adoptive T-cell transfer in nude mice challenged with CaSki/SCT E7 cells, nude mice (3 per group) were inoculated subcutaneously with 1 \times 10⁶ CaSki/SCT E7 tumor cells per mouse. Seven days after tumor challenge, CH containing 5 μ g API-2 or dimethyl sulfoxide was intratumorally injected. One day after hydrogel treatment, mice were either adoptively transferred 1 \times 10⁷ E7-specific CD8⁺ T cells/mouse or intravenously injected with normal saline, as a control.¹⁶ Tumor volumes from CaSki/SCT E7 tumor were recorded regularly for 17 days following immunization. In addition, tumor weight was measured 17 days after tumor challenge.

Western blot. For each experiment, a total of 5 \times 10⁵ cells were rinsed twice with ice-cold phosphate-buffered saline and added 0.2 ml of the protein extraction solution RIPA (Elpis Biotech, Daejeon, Korea) (50 mmol/l Tris Cl, pH 8.0, 150 mmol/l NaCl, 1 mmol/l phenylmethylsulphonyl fluoride, 0.1% sodium dodecyl sulphate, 1% Nonidet P-40 (NP-40), 0.5 mmol/l EDTA). After incubation for 30 minutes on ice, cells were scraped and centrifuged. Protein concentrations were determined by the Coomassie Plus protein assay (Pierce, Rockford, IL). Equal amounts of protein were solubilized in Laemmli buffer (62.5 mmol/l Tris/HCl pH 6.8, 10% glycerol, 2% sodium dodecyl sulphate, 5% mercaptoethanol and 0.00625% bromophenol

blue), boiled for 5 min, and then separated by sodium dodecyl sulphate-polyacrylamide gel electrophoresis and transferred to nitrocellulose membranes (Amersham Bioscience, Uppsala, Sweden). The membranes were probed with primary antibodies diluted 1:1000 for phospho Akt (Ser473), Akt, phospho Erk(T202/Y204), Erk, p38 MAPK, Bcl-w, Bid, Bim, Bad, phospho Bad (Ser 136) (1:1000, Cell Signaling, Beverly, MA), Dual phospho p38 MAPK (1:1000, Stressgen, Victoria, Canada), Bcl-2, cIAP-2, Bcl-xL, Bax, HA-Probe, survivin (1:1000, Santa Cruz Biotechnology, Santa Cruz, CA), Bak (1:1000, BD Biosciences) and E7 (provided by Dr Ju-hong Jun, Seoul National University, Korea) in Tris-buffered saline-T containing 5% bovine serum albumin (Santa Cruz Biotechnology) at 4°C overnight and followed by 3 washes in Tris-buffered saline-T. The membranes were incubated with the appropriate secondary antibodies for 1 hour at room temperature and washed. Immunoreactive bands were visualized by enhanced chemiluminescence (Elpis Biotech, Daejeon, Korea) reaction.

API-2 loaded CH. As a depot system of API-2 (an Akt inhibitor), CH was prepared as described previously.¹³ Briefly, chitosan solution (MW 161 kDa, viscosity 200,000 cps and degree of deacetylation 80%) was obtained by dissolving 40 mg of chitosan in 1.8 ml of 0.1 mol/l HCl solution. Two gram of Glycerol 2-phosphate disodium salt hydrate (β -GP), 5 μ g of API-2 or dimethyl sulfoxide was dissolved in 0.1 ml of distilled water. The chitosan solution was cooled to 4°C and continuously stirred while adding 0.1 ml of mixed solution and the final volume was brought to 2 ml with the addition of distilled water. The final concentration of chitosan in the mixture was 2% wt/vol and was subcutaneously injected into the mice. The mice did not demonstrate severe side effects and maintained a healthy appearance after implantation of the hydrogel.

Statistical analysis. All data are representative of at least two separate experiments. Results for intracellular cytokine staining with flow cytometry analysis, and tumor treatment experiments were evaluated by analysis of variance. Comparisons between individual data points were made using Student's *t*-test. All *P* values <0.05 were considered statistically significant.

SUPPLEMENTARY MATERIAL

Figure S1. Characterization of MHC class I expression of the various subclones derived from P3 tumors.

Figure S2. Characterization of apoptotic cell death of TC-1/no insert and TC-1/CA Akt cells induced by adoptively transferred E7-specific CD8⁺ T cells *in vivo*.

Figure S3. Inactivation of Akt renders a human cancer cell sensitive to CTL-induced apoptosis *in vitro* and *in vivo*.

Figure S4. A17 tumor cells are resistant to chemotherapy and irradiation through the Akt pathway.

ACKNOWLEDGMENTS

This work was supported by the National Cancer Institute SPORE in Cervical Cancer P50 CA098252, 1 RO1 CA114425-01 in the United States as well as a grant R11-2005-017-03003-0 from the Research Center for Women's Diseases of KOSEF, a grant from the National R&D Program for Cancer Control, Ministry of Health & Welfare (070355) and a grant from the Innovative Research Institute for Cell Therapy, Republic of Korea (A062260).

REFERENCES

- Rosenberg, SA, Yang, JC and Restifo, NP (2004). Cancer immunotherapy: moving beyond current vaccines. *Nat Med* **10**: 909–915.
- Lin, KY, Guarnieri, FG, Staveley-O'Carroll, KF, Levitsky, HI, August, JT, Pardoll, DM *et al.* (1996). Treatment of established tumors with a novel vaccine that enhances major histocompatibility class II presentation of tumor antigen. *Cancer Res* **56**: 21–26.
- Wu, TC (2007). The role of vascular cell adhesion molecule-1 in tumor immune evasion. *Cancer Res* **67**: 6003–6006.
- Wu, TC, Guarnieri, FG, Staveley-O'Carroll, KF, Viscidi, RP, Levitsky, HI, Hedrick, L *et al.* (1995). Engineering an intracellular pathway for major histocompatibility complex class II presentation of antigens. *Proc Natl Acad Sci USA* **92**: 11671–11675.
- Lin, KY, Lu, D, Hung, CF, Peng, S, Huang, L, Jie, C *et al.* (2007). Ectopic expression of vascular cell adhesion molecule-1 as a new mechanism for tumor immune evasion. *Cancer Res* **67**: 1832–1841.

6. Kim, S, Jee, K, Kim, D, Koh, H and Chung, J (2001). Cyclic AMP inhibits Akt activity by blocking the membrane localization of PDK1. *J Biol Chem* **276**: 12864–12870.
7. Kohn, AD, Summers, SA, Birnbaum, MJ and Roth, RA (1996). Expression of a constitutively active Akt Ser/Thr kinase in 3T3-L1 adipocytes stimulates glucose uptake and glucose transporter 4 translocation. *J Biol Chem* **271**: 31372–31378.
8. Yang, L, Dan, HC, Sun, M, Liu, Q, Sun, XM, Feldman, RI *et al.* (2004). Akt/protein kinase B signaling inhibitor-2, a selective small molecule inhibitor of Akt signaling with antitumor activity in cancer cells overexpressing Akt. *Cancer Res* **64**: 4394–4399.
9. West, KA, Castillo, SS and Dennis, PA (2002). Activation of the PI3K/Akt pathway and chemotherapeutic resistance. *Drug Resist Updat* **5**: 234–248.
10. Kim, TJ, Lee, JW, Song, SY, Choi, JJ, Choi, CH, Kim, BG *et al.* (2006). Increased expression of pAKT is associated with radiation resistance in cervical cancer. *Br J Cancer* **94**: 1678–1682.
11. Hahnel, PS, Thaler, S, Antunes, E, Huber, C, Theobald, M and Schuler, M (2008). Targeting AKT signaling sensitizes cancer to cellular immunotherapy. *Cancer Res* **68**: 3899–3906.
12. Cheng, JQ, Lindsley, CW, Cheng, GZ, Yang, H and Nicosia, SV (2005). The Akt/PKB pathway: molecular target for cancer drug discovery. *Oncogene* **24**: 7482–7492.
13. Han, HD, Song, CK, Park, YS, Noh, KH, Kim, JH, Hwang, T *et al.* (2008). A chitosan hydrogel-based cancer drug delivery system exhibits synergistic antitumor effects by combining with a vaccinia viral vaccine. *Int J Pharm* **350**: 27–34.
14. Kim, D, Kim, S, Koh, H, Yoon, SO, Chung, AS, Cho, KS *et al.* (2001). Akt/PKB promotes cancer cell invasion via increased motility and metalloproteinase production. *Faseb J* **15**: 1953–1962.
15. Huang, CH, Peng, S, He, L, Tsai, YC, Boyd, DA, Hansen, TH *et al.* (2005). Cancer immunotherapy using a DNA vaccine encoding a single-chain trimer of MHC class I linked to an HPV-16 E6 immunodominant CTL epitope. *Gene Ther* **12**: 1180–1186.
16. Wang, TL, Ling, M, Shih, IM, Pham, T, Pai, SI, Lu, Z *et al.* (2000). Intramuscular administration of E7-transfected dendritic cells generates the most potent E7-specific anti-tumor immunity. *Gene Ther* **7**: 726–733.
17. Hung, CF, Cheng, WF, He, L, Ling, M, Juang, J, Lin, CT *et al.* (2003). Enhancing major histocompatibility complex class I antigen presentation by targeting antigen to centrosomes. *Cancer Res* **63**: 2393–2398.
18. Cheng, WF, Hung, CF, Chai, CY, Hsu, KF, He, L, Ling, M *et al.* (2001). Tumor-specific immunity and antiangiogenesis generated by a DNA vaccine encoding calreticulin linked to a tumor antigen. *J Clin Invest* **108**: 669–678.
19. Chen, CH, Wang, TL, Hung, CF, Yang, Y, Young, RA, Pardoll, DM *et al.* (2000). Enhancement of DNA vaccine potency by linkage of antigen gene to an HSP70 gene. *Cancer Res* **60**: 1035–1042.
20. Hung, CF, Cheng, WF, Hsu, KF, Chai, CY, He, L, Ling, M *et al.* (2001). Cancer immunotherapy using a DNA vaccine encoding the translocation domain of a bacterial toxin linked to a tumor antigen. *Cancer Res* **61**: 3698–3703.